

Velocity Performance Indexes for Parallel Mechanisms with Actuation Redundancy

SEBASTIEN KRUT, OLIVIER COMPANY, FRANÇOIS PIERROT
LIRMM, UMR 5506
CNRS - Université Montpellier II
161, rue Ada
34392 Montpellier Cedex 5, France
<krut, company, pierrot>@lirmm.fr

Abstract: This paper analyses the velocity isotropy of Parallel Mechanism with Actuation Redundancy. The limits of classical indexes based on the Jacobean matrix condition number are shown. Two new indexes are proposed, and the ways to compute them efficiently are given.

1 Introduction

When designing a machine, optimization processes are often run aiming at pointing out the machine of “best performances”. For this task, quality indexes are used. According to the machine purpose, one index is selected, and that will lead to the machine which provides the best score, *i.e.* which offers the best index value. Actually, optimization is often more delicate and often ends with a compromise of several abilities because of the antagonist evolution of various abilities that are essential to the correct behavior of the mechanism.

Among all the quality indexes, the Jacobean matrix condition number is often used; it is supposed to characterize the velocities isotropy of the mechanism. Due to the forces-velocities duality, it is also said to be representative of forces isotropy. The mathematical basics which are the foundations of the isotropy concept for robots have been first defined for serial robots [1][2], and it turns out that a deeper analysis is required when considering more complex mechanisms.

This paper aims at offering such an analysis of isotropy concept when considering PMAR (**P**arallel **M**echanisms with **A**ctuation **R**edundancy), *i.e.* mechanisms where a given operational force does not correspond to a unique set of joint forces. This type of redundancy differs from the kinematic redundancy case where a given operational velocity does not correspond to a unique set of joint velocities. It has been shown [3][4] that actuation redundancy may help to overcome over-mobility singularities, and it seems important to offer tools to correctly analyze the velocity performances of such machines.

In section 2, some basic issues related to condition number are firstly recalled and one of its important limitations is pointed out when considering PMAR: this index does not provide a proper measure of kinematic isotropy. Section 3 is dedicated to the definition of a new index which is consistent with the classical condition number since it refers to measures made on a velocity ellipsoid; however this ellipsoid is rather different from the usual one. Two different algorithms are given: one is based on derivations made in joint space, and the other one on derivations made in operational space. Section 4 is a discussion about different possible indexes and the relevant algorithms: they are based on an analysis of the velocity polytop.

2 Condition number and its application to PMAR

In the following a mechanism is characterized by its inverse Jacobean, \mathbf{J}_m , which links joints velocities $\dot{\mathbf{q}}$ to operational speed, $\dot{\mathbf{x}}$, as follows¹:

$$\dot{\mathbf{q}} = \mathbf{J}_m \dot{\mathbf{x}} \quad (1)$$

2.1 Is a two-dof X-Y table an isotropic device?

In order to illustrate the following discussion, let us consider the simple case of a serial 2-dof X-Y table in fig. 1.

For this mechanism, \mathbf{J}_m is the identity matrix, and for the robotics community, this mechanism is often considered as perfectly isotropic; that is to say, velocity performances are said to be identical in all directions of the operational space. This is clearly not true, as shown in fig. 2 and fig. 3.

¹ The notation $\dot{\mathbf{x}}$ does not mean it is the derivative of operational position vector with respect to time.

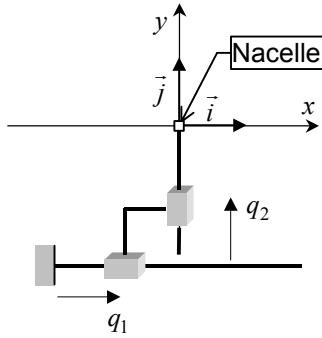


fig. 1 – X-Y table geometry

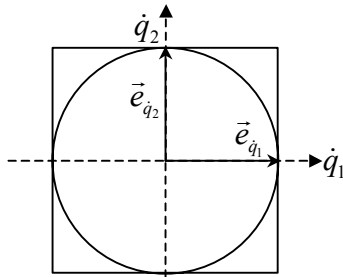


fig. 2 – Reachable joint space of the X-Y table

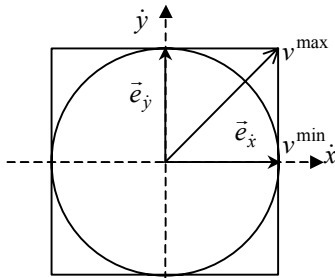


fig. 3 – Reachable operational space of the X-Y table

Reachable joint velocity space is actually a square defined by $|\dot{q}_i| \leq \dot{q}^{\max}$. This square remains a square once mapped in the operational space, using matrix \mathbf{J}_m^{-1} . Therefore the highest velocity reachable by the nacelle is $v^{\max} = \sqrt{2} \times \dot{q}^{\max}$. Such a speed is only accessible for a very specific motion direction. Moreover, $v^{\min} = \dot{q}^{\max}$ is always reachable for all operational directions. Graphically, this results in the circle of radius v^{\min} inscribed in the square. This circle is the image of the joint space circle of radius \dot{q}^{\max} by the linear mapping represented by matrix \mathbf{J}_m^{-1} . Interestingly enough, even if this is not an isotropic device strictly speaking, designers often refer to the deformation of a velocity joint space circle (or hyper-sphere for higher orders) by the Jacobean matrix to measure the “quality” of velocity mapping in terms of isotropy...

2.2 Analysis of a basic non-redundant parallel mechanism

The simple parallel mechanism in fig. 4 is made of two connecting rods linking two identical linear motors to the nacelle. Obviously, the nacelle can move in translation along two directions.

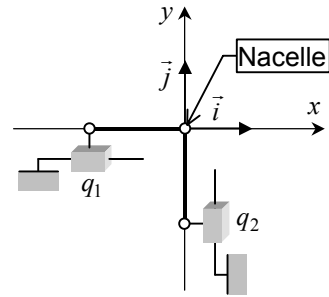


fig. 4 – V shape mechanism geometry

The inverse Jacobean matrix \mathbf{J}_m of this mechanism in this centered position is the same as for the X-Y table (joint and operational reachable domains are those represented in fig. 2 and fig. 3). When the mechanism is not more in its centered position, the inverse Jacobean matrix is not equal to the identity matrix anymore; so if the reachable joint domain remains the same, the reachable operational domain becomes a polytop (see fig. 5).

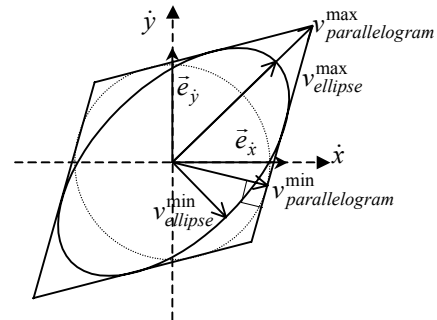


fig. 5 – Reachable operational space for a simple parallel mechanisms.

The image of the joint circle is an ellipse inscribed in the polytop. This ellipse is entirely characterized by the SVD² of \mathbf{J}_m ; the SVD provides in particular the lengths of the ellipse’s axes. A usual isotropy index is derived as the ratio of extreme operational velocities: $v_{ellipse}^{\max}$ and $v_{ellipse}^{\min}$; this index is a measure of the ellipse’s distortion. The lower the distortion is (index value close to 1), the more the ellipse tends towards the circle, considered as the “ideal case” from the isotropy point of view.

Rather than considering the ellipse, one could be interested in the more realistic polytop that may be analyzed in terms of

² Singular Value Decomposition

ratio between the absolute maximal speed ($v_{parallelogram}^{\max}$) and the maximum speed that the mechanism can reach in all operational space directions ($v_{parallelogram}^{\min}$). The latter graphically corresponds to the radius of the largest circle inscribed in the operational polytop.

In this paper, discussions related to PMAR are made for both cases, velocity ellipsoid and velocity polytop; however, the usual inverse Jacobean matrix condition number cannot be used straightforward, as shown in the next section.

2.3 A basic PMAR – 3 actuators / 2 dof

Let us consider the PMAR in fig. 6., made up of three connecting rods and three identical linear actuators. Here, two actuators are colinear.

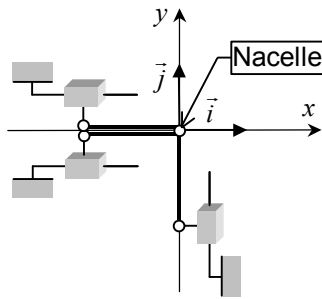


fig. 6 – Geometry of a specific PMAR

This mechanism produces in term of velocities the same effects that the former non-redundant parallel mechanism (fig. 4). So, in this centered position, this mechanism is as isotropic from the velocity point of view as the previous mechanism or even the X-Y table; operational velocities explore the same field as previously: a square (fig. 3).

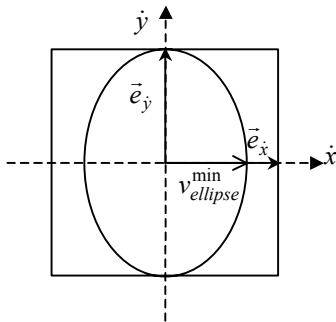


fig. 7 – Reachable operational space for this specific PMAR

For this mechanism the inverse Jacobean matrix, \mathbf{J}_m , is given by:

$$\mathbf{J}_m = \begin{bmatrix} 1 & 0 \\ 1 & 0 \\ 0 & 1 \end{bmatrix}$$

... and its condition number is equal to $\sqrt{2}$. Thus, the ratio between extreme singular values does not represent anymore the ratio of extreme dimensions of the ellipse of maximum surface inscribed in the operational polytop, since this ratio should be equal to 1. Indeed, the operational ellipse obtained using the SVD, has two half-axes which length are \dot{q}_{\max} and $\dot{q}_{\max} / \sqrt{2}$ as depicted in fig. 7.

In different words, the usual isotropy index says such a machine is far from being isotropic, when a common sense analysis says it is as isotropic as an X-Y table. Indeed in such cases, the condition number may give a rough estimate of the anisotropy in force (in reality the machine maximum force along x is twice the maximum force along y), but it does not represent anything related to velocity isotropy.

As a matter of fact, for PMAR the “duality” between force and velocity does not hold anymore for this simple fact: a set of joint forces can be chosen freely within the actuators capacity boundaries, while the components of the joint velocities vector must respect kinematic constraints and thus cannot be chosen freely.

In order to be consistent with the interpretation of the condition number established for non-redundant mechanisms, the ellipse of larger surface inscribed into the operational polytop will be determined. Its characteristics, length of the largest and the smallest half-axis, will lead to a more significant isotropy index which can cope with PMAR.(section 3). Moreover, the way to establish the extreme velocities related to the operational space polytop will be described as well (section 4).

3 Construction of an isotropy index based on ellipses

3.1 Preliminary remarks

- To be simple, different domains of space will be named circle, ellipse, polytop, square, cube. One should keep in mind that those terms must be generalized when considering spaces whose dimensions are higher than 2 or 3 (hyper-circle, hyper-ellipse, and so on).
- Only a-dimensional problems are considered here. In other cases, weighting matrices, $\mathbf{W}_{\dot{x}}$ and $\mathbf{W}_{\dot{q}}$, can be used as follows [9]:

$$\mathbf{W}_{\dot{x}} = \begin{bmatrix} 1/\dot{x}_1^{\max} & & 0 \\ & \ddots & \\ 0 & & 1/\dot{x}_n^{\max} \end{bmatrix}, \tilde{\mathbf{x}} = \mathbf{W}_{\dot{x}} \dot{\mathbf{x}}, |\tilde{x}_i| \leq 1,$$

$$\mathbf{W}_{\dot{q}} = \begin{bmatrix} 1/\dot{q}_1^{\max} & & 0 \\ & \ddots & \\ 0 & & 1/\dot{q}_n^{\max} \end{bmatrix}, \tilde{\mathbf{q}} = \mathbf{W}_{\dot{q}} \dot{\mathbf{q}}, |\tilde{q}_i| \leq 1.$$

Weighting matrices help in managing issues such as: non-homogeneity (coexistence of linear and angular velocities),

differences in actuators' performances ($\dot{q}_i^{\max} \neq \dot{q}_j^{\max}$), differences in desired performances along various operational axes ($\dot{x}_i^{\max} \neq \dot{x}_j^{\max}$).

- The next sub-sections are organized as follows: (i) in section 3.2 linear algebra tools are briefly recalled and the limits of their use for PMAR is pointed out; (ii) in section 3.3, a way to compute the largest admissible ellipse included in the joint polytop and to map it into the operational space is proposed; (iii) in section 3.4 it is proven that the resulting ellipse is actually the largest one in the operational space.

3.2 Analysis of the SVD for a redundant mechanism

For illustration purpose the planar mechanism shown in fig. 8 will be used here. It is a 3 actuators / 2 dof PMAR, which geometry is more general than the one in section 2.3. However, formulas will be established for any type of joint and operational spaces, as long as they respect the following condition:

$$m > n, \text{ with } \dim(\dot{\mathbf{q}}) = m \text{ and } \dim(\dot{\mathbf{x}}) = n$$

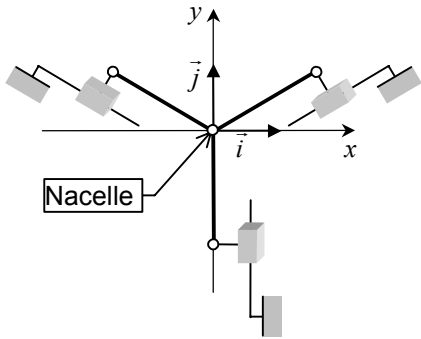


fig. 8 – Geometry of a typical parallel redundant mechanism

The SVD of the inverse Jacobean matrix gives [5]:

$$\mathbf{J}_m = \mathbf{U} \mathbf{S} \mathbf{V}^T, \quad (2)$$

where:

- \mathbf{V}^T is a $n \times n$ orthogonal matrix, representing a linear application in the operational space;
- \mathbf{S} is a rectangular matrix whose upper part includes the singular values of \mathbf{J}_m , $\sigma_1, \dots, \sigma_n$:

$$\mathbf{S} = \begin{bmatrix} \sigma_1 & & 0 \\ & \ddots & \\ 0 & & \sigma_n \\ & & & 0 \end{bmatrix}$$

(Dimensions: n columns, n rows for the upper part, m rows total)

It characterizes the linear application that links a operational velocity vector to a joint velocity vector.

- \mathbf{U} is a $m \times m$ orthogonal matrix, representing a linear application in the joint space. The n first columns, vectors U_1, \dots, U_n ($n < m$) span the range of \mathbf{J}_m . The $m - n$ following columns correspond to the actuators velocities which can never be produced by a movement of the nacelle. They span the kernel of \mathbf{J}_m .

$$\mathbf{U} = \begin{bmatrix} U_1 & \dots & U_n & \dots & U_m \end{bmatrix}$$

(Dimensions: m columns, m rows)

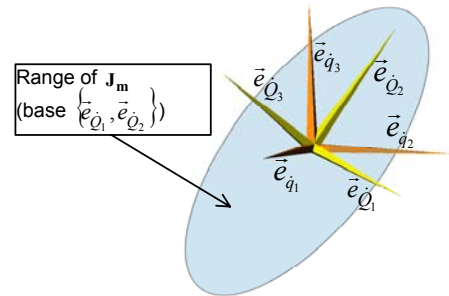


fig. 9 – Graphical representation of $\dot{\mathbf{q}} = \mathbf{U} \tilde{\mathbf{Q}}$

To be acceptable, *i.e.* to be admissible by the mechanism, a joint velocity vector must belong to the range of \mathbf{J}_m . Let us note:

- $\{\tilde{e}_{\dot{q}_1}, \dots, \tilde{e}_{\dot{q}_n}\}$, a base for this type of vector;
- $\tilde{\mathbf{Q}}$ ($\dim(\tilde{\mathbf{Q}}) = n$), a column matrix representative of the joint velocity vector in this base;
- \mathbf{S}_1 , a matrix representing a mapping from the operational space to the restriction of the joint space to the range of \mathbf{J}_m :

$$\mathbf{S}_1 = \begin{bmatrix} \sigma_1 & & 0 \\ & \ddots & \\ 0 & & \sigma_n \end{bmatrix}$$

(Dimensions: n columns, n rows)

The following equation links an admissible joint velocity vector to an operational velocity vector:

$$\dot{\mathbf{x}} = \mathbf{V} \mathbf{S}_1^{-1} \tilde{\mathbf{Q}} \quad (3)$$

The restriction of the unit sphere to the range of \mathbf{J}_m is a circle of radius 1 (*cf.* fig. 10). This circle if transformed into an ellipse in the operational space; the ellipse's half-axes length

are $1/\sigma_i, i \in \{1, \dots, n\}$. The condition number of \mathbf{J}_m is an image of this ellipse's shape.

Obviously, the entire acceptable joint space is not a sphere but a cube defined by the following inequalities:

$$-1 \leq \dot{q}_i \leq 1, i \in \{1, \dots, m\}$$

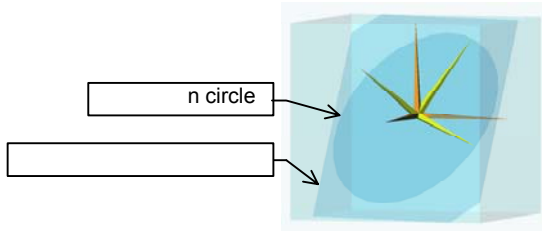


fig. 10 – Intersection of the unit cube and the unit sphere with the range of \mathbf{J}_m

The restriction of this cube to the range of \mathbf{J}_m (cf. fig. 10) is a polygon, or polytop. All acceptable actuator velocity vectors must be located inside this polygon. In fig. 11, the circle and the polygon are depicted. It is to be noted that the circle could be larger and still acceptable because it is not tangent with the polygon. *That implies that the opposite of the singular values are not enlightening maximum speeds which can be reached by the nacelle.*



fig. 11 – Joint polygon and circle

For a non-redundant mechanism, the joint circle and the operational ellipse are the greatest ellipses respectively included into the joint square and the operational polytop; for a PMAR, this is no more the case.

It is proposed in this paper to determine the largest ellipse included in the operational polytop. The ratio of the extreme half-axes of this ellipse can be a really significant isotropy index.

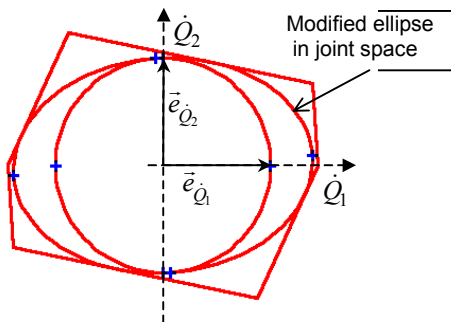


fig. 12 – Joint velocities for a PMAR

Furthermore, it is proposed as well to consider another index constituted from the ratio between the extreme velocities measured at the polytop level, $v_{polytop}^{max}$ and $v_{polytop}^{min}$.

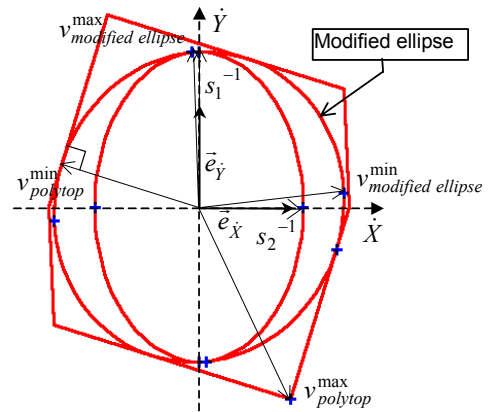


fig. 13 – Operational velocities for a PMAR

Case study

The complete situation is depicted in fig. 14 for a given geometry [120° between each actuators, length of arms = 100, position of the nacelle (-40,-10)].

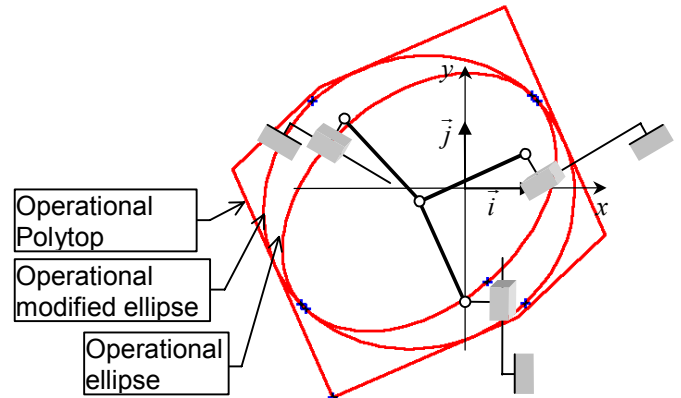


fig. 14 – Operational velocity situation centered on the nacelle.

The obtained results are given in table 1. Clearly the modified operational ellipse is a better representation of the machine velocity capability than the ellipse associated with the restriction of joint space unit sphere (operational ellipse in fig. 14).

$cond(\mathbf{J}_m)$	1.49
Largest ellipse index	1.08
$v_{modified\ ellipse}^{max}$	$1.35 \times \dot{q}_{max}$
$v_{modified\ ellipse}^{min}$	$0.97 \times \dot{q}_{max}$
Polytop index	1.48

table 1 – Results and indexes values

The following sub-sections are dedicated to the derivation of both indexes in a general case.

3.3 Search of the operational ellipse of greatest surface included into the admissible operational polytop

This search can be made:

- by reasoning in joint space, i.e. finding the largest ellipse in joint space and then mapping it into the operational space (section 3.3.1);
- by reasoning directly in the operational space (section 3.3.2).

3.3.1 Reasoning in joint space

The application which transforms the joint unitary circle of the subspace image of \mathbf{J}_m into the joint ellipse of largest surface included in the joint polytop will be determined here. This ellipse, once mapped into the operational space by the linear application of matrix \mathbf{S}_1^{-1} gives the ellipse of largest surface included into the operational polytop (this point will be proved in section 3.3.2). The conditions which must be respected by the joint ellipse to be located inside the joint polytop will be firstly presented; then the conditions to find the largest ellipse will be formulated as an optimization problem.

General approach

Let M be a point of the range of \mathbf{J}_m and belonging to the unitary circle. Vector \overline{OM} (where O is the origin of the frame) is a linear combination of vectors $\vec{e}_{\dot{Q}_1}, \dots, \vec{e}_{\dot{Q}_n}$. Let \mathbf{M} be the column matrix representative of this vector in the base of the range $B_{\text{Im}(\mathbf{J}_m)} = (\vec{e}_{\dot{Q}_1}, \dots, \vec{e}_{\dot{Q}_n})$. The relation $\|\overline{OM}\| = 1$ results in:

$$\mathbf{M}^T \mathbf{M} = 1. \quad (4)$$

The largest ellipse in joint space is calculated with two transformations: (i) the original unitary circle is expanded (point M is transformed in point \tilde{M}), (ii) the expanded ellipse is rotated (point \tilde{M} is transformed in point M'). Thus:

- \tilde{M} belongs to an ellipse whose axis are the vectors of $B_{\text{Im}(\mathbf{J}_m)}$, and whose half-axes length are d_1, \dots, d_n . The column matrix representative of point \tilde{M} in frame of origin O and base $B_{\text{Im}(\mathbf{J}_m)}$, is noted $\tilde{\mathbf{M}}$, and verifies:

$$\tilde{\mathbf{M}} = \mathbf{D} \mathbf{M} \quad (5)$$

where $\mathbf{D} = \text{diag}(d_1, \dots, d_n)$.

- M' belongs to the ellipse of greatest surface. \mathbf{M}' , the matrix associated to point M' verifies:

$$\mathbf{M}' = \mathbf{R} \tilde{\mathbf{M}}, \quad (6)$$

with \mathbf{R} an orthogonal matrix.

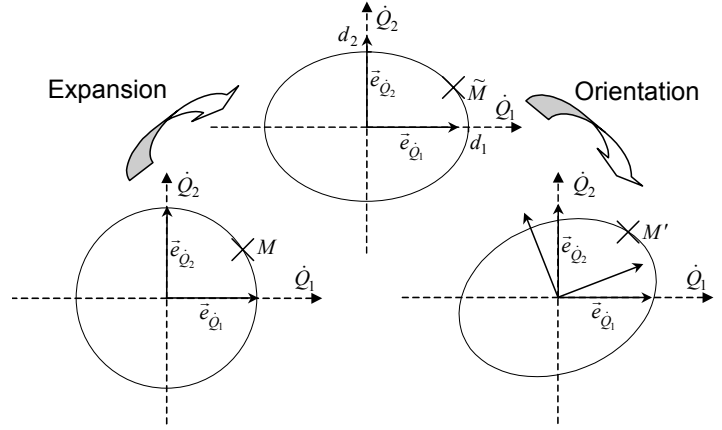


fig. 15 – From the unitary circle to the largest ellipse

Expansion and orientation are combined to get the largest ellipse. To be included in the joint polytop, the ellipse must verify:

- the ellipse is located inside the unitary cube,
- it belongs to the range of \mathbf{J}_m (true by construction).

To belong to the joint cube, point M' must respect the following condition:

$$\vec{e}_{\dot{q}_i} \cdot \overline{OM'} \leq 1 \quad i = 1, \dots, m$$

Indeed, the cube is defined by $2m$ faces. However, the problem is symmetric with respect to point O , and only m faces have to be considered. Such faces are directed by vectors $\vec{e}_{\dot{q}_i}$, $i \in \{1, \dots, m\}$, of the joint space canonic base. This expresses the fact that M' belongs to the i^{th} admissible domain of space, delimited by the plane perpendicular to $\vec{e}_{\dot{q}_i}$, such that the distance from point O to the plane is equal to 1. This can be written in matrix form as follows:

$$\mathbf{E}_i^T \mathbf{M}' \leq 1, \quad (7)$$

where \mathbf{E}_i is the column matrix associated to vector $\vec{e}_{\dot{q}_i}$ in base $B_{\text{Im}(\mathbf{J}_m)} = (\vec{e}_{\dot{Q}_1}, \dots, \vec{e}_{\dot{Q}_n})$.

Finding the vectors perpendicular to the ellipse and the polytop

To guarantee that all ellipse points belong to the i^{th} admissible domain, it is sufficient to verify that the point closest to the i^{th} face is inside this domain. For such a point, the vector \vec{n}'

perpendicular to the ellipse, is collinear to the vector $\vec{e}'_{\dot{q}_i}$, perpendicular to the considered face of the polytop (cf. fig. 16).

Let be $\vec{e}'_{\dot{q}_i}$ the projection of vector $\vec{e}_{\dot{q}_i}$ in the range of \mathbf{J}_m . Because $B_{\text{Im}(\mathbf{J}_m)}$ does only direct a subpart of the articular space it has to be noticed that \mathbf{E}_i is also the column matrix associated to vector $\vec{e}'_{\dot{q}_i}$.

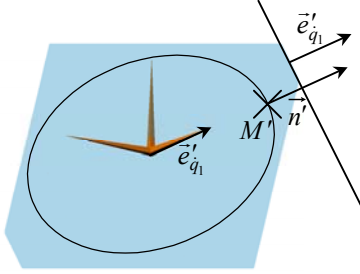


fig. 16 – Colinearity normal to the ellipse / normal to the frontier

The colinearity relationship is expressed as:

$$\exists k / \mathbf{N}' = k \times \mathbf{E}_i, \quad (8)$$

where:

- \mathbf{N}' is the column matrix associated to vector \vec{n}' in base $B_{\text{Im}(\mathbf{J}_m)}$,
- \mathbf{E}_i is the column matrix associated to vector $\vec{e}'_{\dot{q}_i}$.

Let point \tilde{M} be defined in the frame $\langle O, B_{\text{Im}(\mathbf{J}_m)} \rangle$ by the following set of coordinates:

$$(x_1, \dots, x_n)$$

Then the ellipse whose axis are the vectors of $B_{\text{Im}(\mathbf{J}_m)}$, and whose half-axes length are d_1, \dots, d_n is defined by:

$$f(\tilde{M}) = \frac{x_1^2}{d_1^2} + \dots + \frac{x_n^2}{d_n^2} - 1 = 0$$

And the vector perpendicular to the ellipse at point \tilde{M} , \vec{n} , is defined by:

$$\vec{n} = [\overrightarrow{\text{grad} f}](\tilde{M}) = \frac{2}{d_1^2} x_1 \vec{e}_{\dot{Q}_1} + \dots + \frac{2}{d_n^2} x_n \vec{e}_{\dot{Q}_n}.$$

With matrix in base $B_{\text{Im}(\mathbf{J}_m)}$, this results in relation:

$$\tilde{\mathbf{N}} = \mathbf{D}^{-2} \tilde{\mathbf{M}}. \quad (9)$$

In fact, because \mathbf{D} is a diagonal matrix, \mathbf{D}^{-2} is defined by:

$$\mathbf{D}^{-2} = \begin{bmatrix} 1/d_1^2 & & 0 \\ & \ddots & \\ 0 & & 1/d_n^2 \end{bmatrix}.$$

Then \vec{n}' is obtained as:

$$\mathbf{N}' = \mathbf{R} \tilde{\mathbf{N}}. \quad (10)$$

with \mathbf{R} a rotation matrix

Defining the admissible ellipses

To summarize the situation, the system of matrix equations to be solved is the following:

$$\forall i \in \{1, \dots, m\}, \quad \left\{ \begin{array}{l} \mathbf{M}^T \mathbf{M} = \mathbf{1} \quad (4) \\ \tilde{\mathbf{M}} = \mathbf{D} \mathbf{M} \quad (5) \\ \mathbf{M}' = \mathbf{R} \tilde{\mathbf{M}} \quad (6) \\ \mathbf{E}_i^T \mathbf{M}' \leq 1 \quad (7) \\ \exists k / \mathbf{N}' = k \times \mathbf{E}_i \quad (8) \\ \tilde{\mathbf{N}} = \mathbf{D}^{-2} \tilde{\mathbf{M}} \quad (9) \\ \mathbf{N}' = \mathbf{R} \tilde{\mathbf{N}} \quad (10) \end{array} \right.$$

(5) and (6) imply that:

$$\mathbf{M}' = \mathbf{R} \mathbf{D} \mathbf{M}. \quad (11)$$

(9) and (10) lead to:

$$\mathbf{N}' = \mathbf{R} \mathbf{D}^{-2} \tilde{\mathbf{M}}, \quad (12)$$

(12) and (5) lead to:

$$\mathbf{N}' = \mathbf{R} \mathbf{D}^{-1} \mathbf{M}. \quad (13)$$

Inverting (13) leads to:

$$\mathbf{M} = \mathbf{D} \mathbf{R}^T \mathbf{N}'. \quad (14)$$

Combining (11) and (7) gives:

$$\mathbf{E}_i^T \mathbf{R} \mathbf{D} \mathbf{M} \leq 1, \quad (15)$$

combining (8) and (14) gives:

$$\exists k / \mathbf{M} = k \times \mathbf{D} \mathbf{R}^T \mathbf{E}_i, \quad (16)$$

combining (16) and (4), knowing that \mathbf{D} is diagonal, can be written as follows:

$$\exists k / k^2 \mathbf{E}_i^T \mathbf{R} \mathbf{D}^2 \mathbf{R}^T \mathbf{E}_i = 1. \quad (17)$$

In the same way, combining (16) and (7) leads to:

$$\exists k / k \mathbf{E}_i^T \mathbf{R} \mathbf{D}^2 \mathbf{R}^T \mathbf{E}_i \leq 1. \quad (18)$$

While making sure that $0 \leq k \mathbf{E}_i^T \mathbf{R} \mathbf{D}^2 \mathbf{R}^T \mathbf{E}_i$, (18) gives:

$$\exists k / k^2 \mathbf{E}_i^T \mathbf{R} \mathbf{D}^2 \mathbf{R}^T \mathbf{E}_i \times \mathbf{E}_i^T \mathbf{R} \mathbf{D}^2 \mathbf{R}^T \mathbf{E}_i \leq 1. \quad (19)$$

Knowing (17), (19) simplifies in the inequality:

$$\mathbf{E}_i^T \boldsymbol{\Sigma} \mathbf{E}_i \leq 1, \quad (20)$$

with $\boldsymbol{\Sigma} = \mathbf{R} \mathbf{D}^2 \mathbf{R}^T$, a symmetrical matrix.

Of course, (20) has to be verified for all $i = 1, \dots, m$.

As a matter of fact, a relation exists between vectors \mathbf{E}_i and matrix \mathbf{U} . Matrix \mathbf{U} can be expressed as follows:

$$\mathbf{U} = [\mathbf{U}_1 \mid \mathbf{U}_2]$$

with:

$$\mathbf{U}_1 = \begin{bmatrix} \vec{e}_{\dot{q}_1} \cdot \vec{e}_{\dot{Q}_1} & \dots & \vec{e}_{\dot{q}_1} \cdot \vec{e}_{\dot{Q}_n} \\ & \dots & \\ \vec{e}_{\dot{q}_m} \cdot \vec{e}_{\dot{Q}_1} & \dots & \vec{e}_{\dot{q}_m} \cdot \vec{e}_{\dot{Q}_n} \end{bmatrix},$$

$$\mathbf{U}_2 = \begin{bmatrix} \vec{e}_{\dot{q}_1} \cdot \vec{e}_{\dot{Q}_{n+1}} & \dots & \vec{e}_{\dot{q}_1} \cdot \vec{e}_{\dot{Q}_m} \\ & \dots & \\ \vec{e}_{\dot{q}_m} \cdot \vec{e}_{\dot{Q}_{n+1}} & \dots & \vec{e}_{\dot{q}_m} \cdot \vec{e}_{\dot{Q}_m} \end{bmatrix}.$$

And since $\mathbf{E}_i = \begin{bmatrix} \vec{e}_{\dot{q}_i} \cdot \vec{e}_{\dot{Q}_1} \\ \vdots \\ \vec{e}_{\dot{q}_i} \cdot \vec{e}_{\dot{Q}_n} \end{bmatrix}$ \mathbf{U}_1 is expressed as follows:

$$\mathbf{U}_1 = \begin{bmatrix} \mathbf{E}_1^T \\ \vdots \\ \mathbf{E}_m^T \end{bmatrix}. \quad (21)$$

Noting $\mathbf{U}_1(i)$ the i^{th} line of matrix \mathbf{U}_1 equation (20) can be rewritten as:

$$\forall i \in \{1, \dots, m\} \mathbf{U}_1(i) \boldsymbol{\Sigma} \mathbf{U}_1(i)^T \leq 1. \quad (22)$$

Finding the largest admissible ellipse

Among all those ellipses respecting (22), the one of maximal surface still have to be found. This problem is described here as an optimization problem.

The surface of an hyper-ellipse equals to:

$$A = k \times \prod_{i=1}^n d_i,$$

with $k = \pi$ for $n = 2$, $k = \frac{4}{3}\pi$ for $n = 3$, etc.

Maximizing A is equivalent to maximizing the product of the ellipse half-axes length. It is also equivalent to minimizing the following expression:

$$-\prod_{i=1}^n d_i^2.$$

It can be seen that the determinant of $\boldsymbol{\Sigma}$ is:

$$\det(\boldsymbol{\Sigma}) = \det(\mathbf{R}) \times \det(\mathbf{D}^2) \times \det(\mathbf{R}^{-1}) = \det(\mathbf{D}^2),$$

so:

$$\det(\boldsymbol{\Sigma}) = \prod_{i=1}^n d_i^2. \quad (23)$$

To conclude, determining the ellipse of greatest surface included in the joint polytop, consists in finding the *symmetrical* matrix $\boldsymbol{\Sigma}$ which verifies:

- $\det(\boldsymbol{\Sigma})$ minimum
- under constraints

$$\mathbf{U}_1(i) \boldsymbol{\Sigma} \mathbf{U}_1(i)^T \leq 1 \quad \forall i \in \{1, \dots, m\}.$$

The eigen value decomposition of the *real symmetric* $\boldsymbol{\Sigma}$ gives:

$$\boldsymbol{\Sigma} = \mathbf{R} \boldsymbol{\Delta} \mathbf{R}^T, \quad (24)$$

with

- \mathbf{R} is the orientation matrix (note that $\mathbf{R}^T = \mathbf{R}^{-1}$),
- $\boldsymbol{\Delta} = \text{diag}(\delta_1, \dots, \delta_n)$,
- $d_i = \sqrt{\delta_i}$.

The knowledge of \mathbf{R} and \mathbf{D} characterizes entirely the ellipse of greatest surface included inside the joint polytop. This matrix is then mapped by matrix \mathbf{S}_1^{-1} to the ellipse of largest surface included in the operational polytop (This point will be proven in next section).

The sought matrix which represents the transformation of a unitary circle in the admissible part of joint space into the largest ellipse included inside the operational space polytop is given by:

$$\mathbf{X} = \mathbf{S}_1^{-1} \mathbf{R} \mathbf{D}$$

The proposed index is then related to singular values of this matrix, e.g. $\text{cond}(\mathbf{X})$, or $\min(\sigma(\mathbf{X}))$, etc.

3.3.2 Reasoning in operational space

Rather than seeking the ellipse of maximum surface included inside the joint polytop, and then computing its image in the operational space, it is possible to find the ellipse of greatest surface included inside the operational polytop.

The following relation describes the mapping between the operational space and the range of \mathbf{J}_m :

$$\mathbf{M}' = \mathbf{S}_1 \mathbf{K}', \quad (25)$$

with:

- $M' \in \text{range}(\mathbf{J}_m)$,
- K' a point in operational space,
- \mathbf{M}' the column matrix associated with M' in $B_{\text{Im}(\mathbf{J}_m)}$,
- \mathbf{K}' the column matrix associated with K' in the singular vectors base.

M' belongs to the joint polytop:

$$\mathbf{E}_i^T \mathbf{M}' \leq 1 \quad i=1, \dots, m. \quad (26)$$

Thanks to relation (25), equation(26) becomes in operational space:

$$\mathbf{E}_i^T \mathbf{S}_1 \mathbf{K}' \leq 1. \quad (27)$$

Since equation (27) is the only equation that differs from the system of equations of the previous section, the resolution of the system leads to:

$$\forall i \in \{1, \dots, m\} \quad \mathbf{U}_1(i) \mathbf{S}_1 \boldsymbol{\Sigma}' \mathbf{S}_1^T \mathbf{U}_1(i)^T \leq 1, \quad (28)$$

where $\boldsymbol{\Sigma}'$ is a symmetrical matrix defined as follows:

$$\boldsymbol{\Sigma}' = \mathbf{R}' \mathbf{D}'^2 \mathbf{R}'^T$$

Those equations express the constraints that must be fulfilled by the operational ellipse to be located inside the operational polytop. Those relations are very similar to those obtained in the joint space.

In the operational space, the optimization problem consists in finding a *symmetrical* matrix $\boldsymbol{\Sigma}'$ which verifies:

- $\det(\boldsymbol{\Sigma}')$ minimum

under constraints

$$\mathbf{U}_1(i) \mathbf{S}_1 \boldsymbol{\Sigma}' \mathbf{S}_1^T \mathbf{U}_1(i)^T \leq 1 \quad \forall i \in \{1, \dots, m\}$$

The eigen values decomposition of $\boldsymbol{\Sigma}'$ leads to matrix \mathbf{R}' and \mathbf{D}' . Matrix $\mathbf{X}' = \mathbf{R}' \mathbf{D}'$ characterizes the linear application that transforms a unitary circle in the ellipse of maximum surface included into the operational polytop. The ratio of extreme diagonal values of \mathbf{D}' constitutes the isotropy index built previously.

One can check that $\mathbf{X} = \mathbf{X}'$, that is to say that the ellipses obtained with both methods are the same. In fact referring to the definitions of \mathbf{X} and \mathbf{X}' , it can be verified that:

$$\boldsymbol{\Sigma} = \mathbf{S}_1 \mathbf{X} \mathbf{X}^T \mathbf{S}_1^T,$$

$$\boldsymbol{\Sigma}' = \mathbf{X}' \mathbf{X}'^T.$$

So the admissible domains constraints can be written as:

- Reasoning in joint space:

$$\mathbf{U}_1(i) \mathbf{S}_1 \mathbf{X} \mathbf{X}^T \mathbf{S}_1^T \mathbf{U}_1(i)^T \leq 1,$$

- Reasoning in operational space:

$$\mathbf{U}_1(i) \mathbf{S}_1 \mathbf{X}' \mathbf{X}'^T \mathbf{S}_1^T \mathbf{U}_1(i)^T \leq 1.$$

In joint space, $-\det(\boldsymbol{\Sigma})$ has to be minimized, that is $-\det(\mathbf{X} \mathbf{X}^T)$, because:

$$-\det(\boldsymbol{\Sigma}) = -2 \det(\mathbf{S}_1) \det(\mathbf{X} \mathbf{X}^T), \\ \det(\mathbf{S}_1) > 0.$$

In operational space $-\det(\boldsymbol{\Sigma}')$ has to be minimized, that is: $-\det(\mathbf{X}' \mathbf{X}'^T)$. Thus, both entities are obtained as results of the same optimization problem under the same constraints.

4 Determination of extreme velocities of the operational polytop

In this section, the extreme velocities of the operational polytop will be determined. The "lowest" velocity is defined as the minimum velocity always reachable by the nacelle in all directions of the operational space. The "highest" velocity is the maximum velocity that can be reached by the nacelle in a very particular direction.

The highest velocity $v_{polytop}^{\max}$ belongs necessarily to a vertex of the polytop; the lowest value $v_{polytop}^{\min}$ is located on one of the faces (cf. fig. 13).

Finding $v_{polytop}^{\max}$

Referring to (27), a point K'_i belonging to the i^{th} face can be described by:

$$\mathbf{E}_i^T \mathbf{S}_1 \mathbf{K}'_i = 1, \quad (29)$$

a point K'_{m+i} , $i \in \{1, \dots, m\}$, belonging to the adjacent face (the $(m+i)^{th}$ face) can be described by:

$$-\mathbf{E}_i^T \mathbf{S}_1 \mathbf{K}'_{m+i} = 1. \quad (30)$$

In the optimization problem faces of type (30) have not been considered; here they must be taken into account. A vertex of the polytop is a point of the n -dimensional operational space. The $2m$ frontier equations (m of type (29) and m of type (30)) will be seek, to find all the combinations of n faces which generate a vertex. For this, all C_{2m}^n possible systems will be seeked.

If the i^{th} system can be solved, the fact that point K'_i , $i \in \{1, \dots, 2m\}$ belongs to the polytop will have to be verified. The system might have no solution, for example when two vectors \bar{e}_i et \bar{e}_j have the same projection in the range of \mathbf{J}_m : $\mathbf{E}_i = \mathbf{E}_j$. Moreover, when a point K'_i is established, this point might be located outside the admissible space (cf. fig. 17).

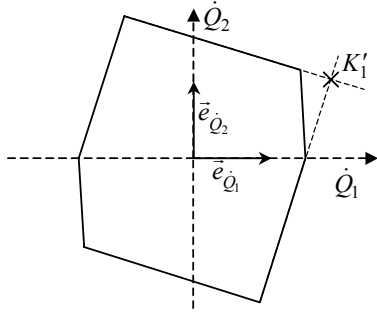


fig. 17 – Determination of a point outside from the admissible polytop

Once all vertices are determined, the highest distance between the center and points K'_i is given by:

$$v_{parallelogram}^{\max} = \max_{i \in \{1, \dots, 2m\}} \|\mathbf{K}'_i\|. \quad (31)$$

Finding $v_{polytop}^{\min}$

The lowest distance $v_{polytop}^{\min}$ is measured between the center and a point located on one of the side of the polytop. Let us note H'_i the closest point on side i . OH'_i is collinear with the normal of this side.

Relation (29) for H'_i and i^{th} face is the following:

$$\mathbf{E}'_i{}^T \mathbf{H}' = 1, \quad (32)$$

where $\mathbf{E}'_i = \mathbf{S}_1 \mathbf{E}_i$ is the normal vector to the side.

The colinearity relation can be written as follows:

$$\exists k / \mathbf{H}'_i = k \mathbf{E}'_i, \quad (33)$$

so, combining (33) and (32) implies:

$$\mathbf{E}'_i{}^T k \mathbf{E}'_i = 1. \quad (34)$$

Thus k is:

$$k = 1 / \|\mathbf{E}'_i\|^2. \quad (35)$$

By replacing the value of k in relation (33) and by calculating the distance from point H'_i , $i \in \{1, \dots, m\}$ to the center, this leads to:

$$\|\mathbf{H}'_i\| = 1 / \|\mathbf{E}'_i\|, \quad (36)$$

that is to say, by using expression of \mathbf{E}'_i :

$$\|\mathbf{H}'_i\| = 1 / \|\mathbf{S}_1 \mathbf{E}_i\|. \quad (37)$$

Then, the sought value is given by:

$$v_{parallelogram}^{\min} = \min_{i \in \{1, \dots, m\}} \|\mathbf{H}'_i\|. \quad (38)$$

5 Conclusion

In this paper we have firstly shown the limits of classical indexes based on the Jacobean matrix condition number when Parallel Mechanisms with Actuation Redundancy are considered in terms of velocity isotropy. We have introduced new tools to analyze and optimize such mechanisms. The first set of tools offers measures based on a classical point of view, a velocity ellipsoid, with an important feature: the sought ellipsoid is much closer to the real machine capability than the one usually considered. The second set of tools is based on velocity polytop: the ways to efficiently compute such a polytop and, more important, its extreme values have been described. It is expected that indexes based on both analysis can be usefully implemented in optimization processes for new redundant parallel mechanisms.

References

- [1] T. Yoshikawa, "Manipulability of robotic mechanisms", in *Robotics Research: The second International Symposium*, eds. H. Hanafusa and H. Inoue, MIT Press, Cambridge (MA), USA, 1985
- [2] T. Yoshikawa, "Dynamic manipulability of robot manipulators", in *Journal of Robotic Systems*, Vol. 2, No. 1, pp. 113-124, 1985.
- [3] F. Marquet, S. Krut, O. Company, F. Pierrot, "Archi, a redundant mechanism for machining with unlimited rotation capacities", in *Proc. of ICAR*, Budapest, Aug. 2001.
- [4] S.J. Ryu, J.W. Kim, J.C. Hwang, C. Park, H.S. ho, K. Lee, Y. Lee, U. Cornel, F.C. Park and J. Kim, "ECLIPSE: An Overactuated Parallel Mechanism for Rapid Machining", in *Proc. ASME Int. Mechanical Engineering Congress and Exposition*, USA, 1998, Vol. 8, pp. 681-689.
- [5] V. C. Klema and A. J. Laub, "The singular value decomposition: its computation and some applications," in *IEEE Transactions and Automatic Control*, Vol. AC-25, No. 2, pp. 164-176, 1980.
- [6] P. Chiacchio, Y. Bouffard-Vercelli and F. Pierrot, "Evaluation of Force Capabilities for Redundant Manipulators", in *Proc. of IEEE ICR&A*, Minneapolis (Minnesota), USA, April 1996.
- [7] F. Pierrot and P. Chiacchio, "Evaluation of Velocity Capabilities for Redundant Parallel Robots", in *Proc. of IEEE ICR&A*, Albuquerque, New Mexico, April 1997.
- [8] J. Kirchner and R. Neugebauer, "How to optimize parallel link mechanisms – proposal of new strategy", in *Proc. of IEEE ICR&A*, Albuquerque, New Mexico, April 1997.

- [9] L. Stocco, S. E. Salcudean and F. Sassani, "Matrix Normalization for Optimal Robot Design", in *Proc. of IEEE ICR&A*, Leuven, Belgium, May 16-21, 1998.
- [10] L. J. Stocco, S. E. Salcudean, F. Sassani, "Mechanism Design for Global Isotropy with Applications to Haptic Interfaces", in *Proc. of ASME Int. Mechanical Engineering Congress and Exhibition*, Vol. 61, pp. 115-122, 1997.
- [11] S. E. Salcudean and L. Stocco, "Isotropy and Actuator Optimization in Haptic Interface Design", in *Proc. of IEEE ICR&A*, San Francisco, CA, USA, April 22-28, 2000.
- [12] C. M. Gosselin and J. Angeles, "A global performance index for the kinematic optimization of robotic manipulators", in *ASME Journal of Mechanical Design*, Vol. 113, No. 3, pp. 220-226, 1991.
- [13] J. Kirchner, R. Neugebauer, "How to Optimize Parallel Link Mechanisms - Proposal of a New Strategy", in *Proc. of 2000-PKM-IC*, Ann Arbor (MI), USA, September 13-15, 2000.
- [14] J. Lee, J. Duffy and K. H. Hunt, "The Optimum Quality Index for Some Spatial In-parallel Devices", in *Proc. of Florida Conference on Recent Advances in Robotics*, Miami (Florida), USA, April 10-11, 1997.